On the analytical construction of halo orbits and halo tubes in the elliptic restricted three-body problem

Rocío I. Paez[1,2] & Massimiliano Guzzo[2]

[1]School of Computer Science and Information Technology, University College Cork UCC, Cork, Ireland

[2]Dipartimento di Matematica "Tullio Levi-Civita", Università degli Studi di Padova

Padova 35122 (PD) Italia

March 31, 2022

Abstract

The halo orbits of the spatial circular restricted three-body problem are largely considered in space-flight dynamics to design low-energy transfers between celestial bodies. A very efficient analytical method for the computation of halo orbits, and the related transfers, has been obtained from the high-order resonant Birkhoff normal forms defined at the Lagrangian points L1-L2. In this paper, by implementing a non-linear Floquet-Birkhoff resonant normal form, we provide the definition of orbits, as well as their manifold tubes, which exist in a large order approximation of the elliptic three-body problem and generalize the halo orbits of the circular problem. Since the libration amplitude of such halo orbits is large (comparable to the distance of L1-L2 to the secondary body), and the Birkhoff normal forms are obtained through series expansions at the Lagrangian points, we provide also an error analysis of the method with respect to the orbits of the genuine elliptic restricted three-body problem.

1 Introduction

In recent years, the scientific exploration of the vicinity of the Lagrangian points, particularly in the Sun-Earth and Earth-Moon systems, has been particularly intense. In particular, the computation of trajectories which are in the manifolds asymptotic to orbits librating close the Lagrangian points L_1-L_2 has gained a high priority for space-flight dynamics: typically, the transfer design has evolved from the familiar Earth-to-orbit concept to an Earth-to-manifold strategy. The halo orbits of the spatial circular restricted three-body problem have been largely considered to design low-energy Earth-to-manifold transfers [7, 8]. For example, a basic halo orbit was incorporated into the trajectory for the International Sun Earth Explorer-3 (ISEE-3) satellite, launched toward a Sun-Earth L_1 halo orbit in 1978 (the satellite was the first to successfully reach a libration point

arXiv:2203.16315v1 [astro-ph.EP] 29 Mar 2022

orbit). Since ISEE-3, several missions to Sun-Earth libration point orbits have been accomplished. A current example is the James Webb Space Telescope (JWST), designed for observations of deep space in the infrared spectrum from an L_2 orbit.

The halo orbits are defined in the Circular Restricted Three-Body Problem (CRTBP) from the computation of large order resonant Birkhoff normal forms at the Lagrangian point L_1 or L_2 [16, 25, 24, 4, 2, 29]. Precisely, the Birkhoff normal forms are used to compute analytically all the orbits in the center manifold of the selected Lagrangian point L_1; therefore, from the Poincaré section of the dynamics restricted to the center manifold one defines the halo orbits. In Figure 1 we represent an example of the output of such a computation: on the left panel we represent the phase portrait of the Poincaré section for a sample value of the reduced mass μ and of the Jacobi constant C, and on the right panel we represent the corresponding halo orbits in space. We emphasize that using the Birkhoff-normal forms, one obtains not only the orbits on the center manifold, but also the orbits which are asymptotic to them and the orbits transiting in its neighbourhood. Thus, they provide a complete analytic framework to study the Earth-to-manifold transfers in the approximation of the CRTBP. The CRTBP is indeed the main model to introduce the dynamics close to L_1, L_2 of a selected secondary body (for example the Earth). Due to their importance for space-flight dynamics, many efforts to use halo orbits in models more complicated than the CRTBP have been done in the literature [11, 13, 21, 22]. For example, in the real Solar System the eccentricity of the orbits of the planet identified as the secondary body, as well as the perturbations from the other planets, limit the study to look for orbits with features similar to the orbits identified in the approximation of the CRTBP (see for example [20, 3, 17, 33, 32, 23, 34]).

When we consider the short time-spans typical of space-flight dynamics or of close encounters of a comet with a planet, the major modification to the CRTBP is represented by the Elliptic Restricted Three-Body Problem (ERTBP), where the orbit of the secondary body P_2 performs an elliptic motion around the primary body P_1. The ERTBP is conveniently represented as a non-autonomous Hamiltonian system having the Lagrangian solutions L_1, L_2 but without a global first integral, such as the Jacobi constant, which is used to define the Poincaré sections and label the halo orbits in the CRTBP. In the paper [28] we have introduced Floquet-Birkhoff normal forms for the ERTBP which allowed us to generalize and compute the families of planar and vertical Lyapunov orbits generating at L_1, L_2, as well as the low-energy transits from one side to the other of the secondary body. In this paper we compute halo orbits for the ERTBP from *resonant* Birkhoff-Floquet normal forms. Despite the lack of a global first integral for the ERTBP, the resonant Birkhoff-Floquet normal form allows us to define a non-linear approximation of large order of the dynamics, with an approximate local first integral, which we call 'local energy', labelling the Poincaré sections close to L_1, L_2. From the Poincaré sections we identify then the halo orbits, which are finally mapped to the Cartesian space using a time-dependent canonical transformation. This method of computation of halo orbits (as well as the method used for the CRTBP) is based on series expansions of the Hamiltonian,

2
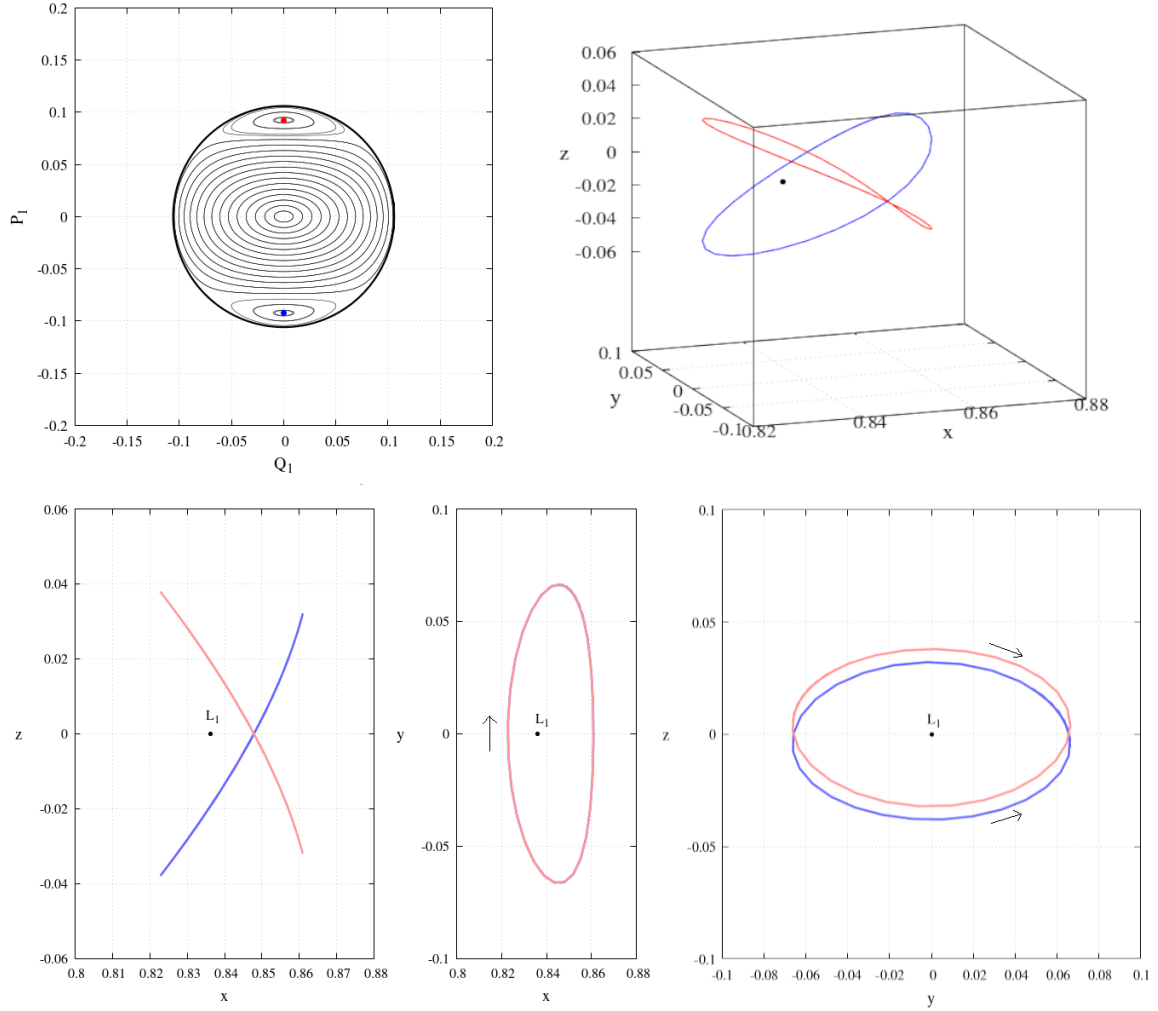
Figure 1: Examples of northern (red) and southern (blue) halo orbits (top-right panel) computed in the CR3BP, for $\mu = 0.0123$ (identifying the Earth-Moon system) and the Jacobi constant $C = 3.1637151$. The top-left panel reports the phase portrait of the Poincaré section (the variables Q_1, P_1 on the section will be defined in Section 4) for the same values of μ, C. In the bottom panels we represent the projection of these halo orbits on the Cartesian planes (the arrows indicate the sense of motion in each case).

truncated at a large order. The dependence of the error on this truncation order is influenced both by the singularity of the Hamiltonian corresponding to a collision with P_2 (see [27]) and by the well known problem of accumulation of small divisors (see for example [5] and references therein). Since the family of halo orbits forms with a minimum libration amplitude, it is necessary to perform a test on the error introduced with the truncation of series.

The paper is organized as follows: in Section 2 we review some basic properties of halo orbits in the CR3BP; in Section 3 we introduce the resonant Floquet-Birkhoff normal forms of the ERTBP, and from these normal forms we define the halo orbits as well as their asymptotic manifolds; in Section 4 we illustrate an application of the method to the Earth-Moon ERTBP, with the error analysis.

2 Halo orbits: from the CR3BP to the ER3BP

The CRTBP is defined by the dynamics of a particle P of infinitesimal mass attracted by two massive bodies P_1, P_2 revolving around their center of mass in circular orbits. In a suitable rotating reference frame this model admits five equilibrium points, the so called Lagrangian points $L_1, \ldots, L_5$, and a first integral, the Jacobi constant, related to the energy of the particle. In this paper we focus on the collinear Lagrangian points L_1, L_2, which behave, linearly, as the product of two centers by a saddle. Due to the center-center part, there are 4-dimensional center manifolds for L_1 and L_2, containing also periodic orbits and invariant KAM tori [1, 18, 26]. It is convenient to consider the 3-dimensional levels of the center manifolds that we obtain when we fix the value of the Jacobi constant; the stable and unstable manifolds of these sets are the so called manifold tubes. The orbits on the manifold tubes approach exponentially orbits on the center manifold in the future (the stable manifold tubes) or in the past (the unstable manifold tubes). From the several types of families of orbits in the center manifolds two families are of particular interest for Astrodynamics: the planar Lyapunov orbits and the three-dimensional halo orbits.

The family of halo orbits results from a bifurcation in the corresponding L_1 or L_2 Lyapunov family [14, 15], and extends from the vicinity of the Lagrangian point toward the nearest massive body P_2. All halo orbits include an out-of-plane component, i.e. an amplitude component in the (vertical) z-direction. In particular, for the L_1 halo family, the vertical amplitude increases as the orbit moves toward P_2. Because the halo family results from a pitchfork bifurcation in the planar family, the bifurcation introduces two branches that extend both above and below the xy-plane. A halo orbit with a maximum out-of-plane excursion in the positive z-direction is termed a northern halo orbit, while the orbits with a maximum vertical amplitude in the negative z-direction is termed southern. A sample northern orbit (red) with the corresponding southern halo (blue) is plotted in Figure 1. Note that from a xy-projection, the direction of motion for both northern and southern orbits about L_1 is clockwise, but when viewed from a yz-projection, the motion of the northern orbit is clockwise while the motion of the southern orbit is counter-clockwise.

The halo orbits of the CRTBP have been analytically computed from computer assisted implementations of Hamiltonian perturbation theory as well as from numerical

4

methods (see for example [16, 25, 4, 29] for the analytic methods and [8, 15, 12, 31, 30] for the numerical ones). In this paper we consider the analytic computations based on Hamiltonian perturbation theory, which allow not only to compute the halo orbits, but also the orbits in their neighbourhoods, including their stable and unstable manifolds and transit orbits. In the CR3BP the result is achieved by computing a resonant Birkhoff normal form of large order N: by neglecting the large order remainder, one remains with and integrable Hamiltonian system which is used to compute the Poincaré section of the Hamiltonian flow on the center manifold, and consequently the halo orbits. We extend these methods to the ERTBP by providing a definition of halo orbits in the elliptic problem, and a method of computation based on the resonant version of the Floquet-Birkhoff normal forms which were introduced in [28]. The resonant Floquet-Birkhoff normal forms will be used to define also the manifolds tubes and the transit motions associated to halo orbits in the ERTBP.

The ERTBP is defined by the motion of a body P of infinitesimally small mass moving in the gravity field generated by two massive bodies P_1 and P_2, which move around their common center of mass according to the elliptic solutions of the two-body problem. It is convenient to represent the motion of P using a rotating-pulsating reference frame (x, y, z) whose origin is in the center of mass of P_1 and P_2, the z axis is orthogonal to their motion, and the x, y axes are rotating-pulsating so that P_1, P_2 remain at fixed locations on the horizontal axis x. With standard units of measure, the Hamiltonian representing the motions of P in this pulsating-rotating frame is

$$
\begin{aligned}
h(x, y, z, p_x, p_y, p_z, f; e) = {} & \frac{p_x^2}{2} + \frac{p_y^2}{2} + \frac{p_z^2}{2} - p_y\, x + p_x\, y \\
& + \frac{1}{1 + e \cos f} \left(\frac{1}{2}\, e\, (x^2 + y^2 + z^2) \cos f \right. \\
& \left. - \frac{\mu}{\sqrt{(x - (1 - \mu))^2 + y^2 + z^2}} - \frac{1 - \mu}{\sqrt{(x + \mu)^2 + y^2 + z^2}} \right) ,
\end{aligned}
\tag{1}
$$

where the independent variable, denoted by f, corresponds to the true anomaly of the secondary body, the parameter $\mu \in (0, \frac{1}{2}]$ denotes the reduced mass, and e denotes the eccentricity of the elliptic motion. The main advantage of using rotating–pulsating variables is that the Hamilton equations of (1) have five equilibrium points $L_1, \ldots, L_5$ located in the same positions $(x_{L_i}, y_{L_i}, 0)$ of the corresponding circular problem; the collinear points L_1, L_2 are denoted by $(x, y, z, p_x, p_y, p_z) = (x_{L_i}, 0, 0, 0, x_{L_i}, 0)$. For each selected equilibrium L_i we first introduce the variables $(\mathbf{q}, \mathbf{p}) = (q_1, q_2, q_3, p_1, p_2, p_3)$:

$$
\begin{aligned}
x &= q_1 + x_{L_i} , & p_x &= p_1 , \\
y &= q_2 , & p_y &= p_2 + x_{L_i} , \\
z &= q_3 , & p_z &= p_3 ,
\end{aligned}
\tag{2}
$$

such that the equilibrium point L_i is in the origin of the phase-space, and consider the Taylor expansion of h in $(\mathbf{q}, \mathbf{p})$:

$$
H(\mathbf{q}, \mathbf{p}, f; e) = H_2 + H_3 + \ldots
\tag{3}
$$

5

where each term $H_j(\mathbf{q}, \mathbf{p}, f; e)$ is a polynomial of degree j in the variables $(\mathbf{q}, \mathbf{p})$. Notice that the zero-order term $H_0(f; e)$ has been removed from the Hamiltonian; the term of order 1 vanishes because we are expanding the Hamiltonian at an equilibrium point; the term of second order is

$$H_2(\mathbf{q}, \mathbf{p}, f; e) = \frac{p_1^2}{2} + \frac{p_2^2}{2} + \frac{p_3^2}{2} - p_2\, q_1 + p_1\, q_2 + \frac{\beta\left(-2q_1^2 + q_2^2 + q_3^2\right)}{1 + e \cos f} + \frac{(e \cos f)\left(q_1^2 + q_2^2 + q_3^2\right)}{2\left(1 + e \cos f\right)} \quad (4)$$

with

$$\beta = \frac{1}{2}\left(\frac{\mu}{|1 - x_{L_i} - \mu|^3} + \frac{1 - \mu}{|x_{L_i} + \mu|^3}\right) . \quad (5)$$

Then, we use a combination of the Floquet theory and Birkhoff normalizations to conjugate the Hamiltonian (3) to a normal form which is autonomous up to a suitable large order N:

$$K(\mathbf{Q}, \mathbf{P}, f; e) = K_2(\mathbf{Q}, \mathbf{P}; e) + K_4(\mathbf{Q}, \mathbf{P}; e) + \ldots + K_N(\mathbf{Q}, \mathbf{P}; e) + R_{N+1}(\mathbf{Q}, \mathbf{P}, f; e) \quad (6)$$

where each term $K_j(\mathbf{Q}, \mathbf{P}; e)$ is an autonomous polynomial of degree j in the variables $(\mathbf{Q}, \mathbf{P})$ and is 1-1 resonant in the sense explained below. The remainder $R_{N+1}(\mathbf{Q}, \mathbf{P}, f; e)$ of the Taylor expansion of K contains monomials from order $N + 1$ and is possibly dependent on f.

To define the resonance properties of the polynomials $K_j(\mathbf{Q}, \mathbf{P}; e)$ it is convenient to introduce the Birkhoff variables $\hat{\mathbf{q}}, \hat{\mathbf{p}}$ canonically conjugated to the real variables $(\mathbf{Q}, \mathbf{P})$ by the linear transformation:

$$Q_3 = \hat{q}_3 \ , \quad P_3 = \hat{p}_3 \ , \quad Q_j = \frac{\hat{q}_j + \mathrm{i}\,\hat{p}_j}{\sqrt{2}} \ , \quad P_j = \frac{\mathrm{i}\,\hat{q}_j + \hat{p}_j}{\sqrt{2}} \ , \quad j = 1, 2. \quad (7)$$

In this paper we consider the resonant Floquet-Birkhoff normal forms such that all the terms $K_j(\mathbf{Q}, \mathbf{P}; e)$, when represented using the variables $\hat{\mathbf{q}}, \hat{\mathbf{p}}$, are the sum of monomials

$$a_{\mathbf{m}, \mathbf{l}} \hat{q}_1^{m_1} \hat{q}_2^{m_2} \hat{q}_3^{m_3} \hat{p}_1^{l_1} \hat{p}_2^{l_2} \hat{p}_3^{l_3}$$

with $m_3 = l_3$ and $(l_1 - m_1) + (l_2 - m_2) = 0$. This means that, if we introduce the action-angle variables $I_1, I_2, \theta_1, \theta_2$ for the elliptic motions and the hyperbolic variables I_3, θ_3 such that:

$$
\begin{aligned}
\hat{q}_1 &= -\mathrm{i}\,\sqrt{I_1}\,\mathrm{e}^{\mathrm{i}\,\theta_1} \ , & \hat{p}_1 &= \sqrt{I_1}\,\mathrm{e}^{-\mathrm{i}\,\theta_1} \ , \\
\hat{q}_2 &= -\mathrm{i}\,\sqrt{I_2}\,\mathrm{e}^{\mathrm{i}\,\theta_2} \ , & \hat{p}_2 &= \sqrt{I_2}\,\mathrm{e}^{-\mathrm{i}\,\theta_2} \ , \\
\hat{q}_3 &= \sqrt{I_3}\,\mathrm{e}^{\theta_3} \ , & \hat{p}_3 &= \sqrt{I_3}\,\mathrm{e}^{-\theta_3} \ ,
\end{aligned}
\quad (8)
$$

the terms K_j are independent of θ_3, and depend on θ_1, θ_2 only through the resonant combination $\theta_1 - \theta_2$.

Remark. In our paper [28] we constructed non-resonant Floquet-Birkhoff normal forms, so that all the terms $K_j(\mathbf{Q}, \mathbf{P}; e)$ were integrable in the sense that, when represented using the variables $\hat{\mathbf{q}}, \hat{\mathbf{p}}$, they depended on the variables only through the combinations $i\hat{q}_1\hat{p}_1$, $i\hat{q}_2\hat{p}_2$ (the actions of the elliptic motions expressed in Birkhoff complex variables) and

$\hat{q}_3\hat{p}_3$ (the action of the hyperbolic motion). This type of normal form, which is specifically designed for the efficient analytic computation of the planar and vertical Lyapunov orbits, as well as their manifold tubes, can be constructed if the three frequencies describing the motion are strictly non resonant up to order N. As pointed in [29], while for the Earth-Moon system ($\mu = 0.0123$) indeed no exact low order resonance takes place, the linear frequencies lay very close to a 1-1 resonance opening the door, for the CRTBP, to the appearance of the halo orbits at suitable large values of the Hamiltonian. Therefore, while very efficient in the context of planar Lyapunov orbits and their manifold tubes, the construction presented in [28] obviously excludes the computation of Halo orbits.

Let us now define the halo orbits in the ERTBP using the resonant Floquet-Birkhoff normal forms (6). Since the dependence on f is relegated within the remainder of the normal form, the definition of the halo orbits as well as of their manifolds tubes in the normal form variables $(\mathbf{Q}, \mathbf{P})$ is obtained as in the CRTBP from the approximated Hamiltonian:

$$\mathcal{K}(\mathbf{Q}, \mathbf{P}; e) = K_2(\mathbf{Q}, \mathbf{P}; e) + K_4(\mathbf{Q}, \mathbf{P}; e) + \ldots + K_N(\mathbf{Q}, \mathbf{P}; e), \qquad (9)$$

which we call *local energy*. Since the Hamiltonian $\mathcal{K}$ is integrable by quadratures, we can compute and classify all the solutions of its Hamilton equations. In particular:

- for $Q_3, P_3 = 0$ we have the center manifold $\mathcal{M}$ of the equilibrium $(\mathbf{Q}, \mathbf{P}) = (0, \ldots, 0)$ for the Hamiltonian flow of $\mathcal{K}$; we denote by $\mathcal{M}_\kappa$ the intersection of the center manifold $\mathcal{M}$ with the level set $\mathcal{K}(\mathbf{Q}, \mathbf{P}; e) = \kappa$ of the local energy;

- for $Q_3 = 0, P_3 \neq 0$ and for $Q_3 \neq 0, P_3 = 0$ we have the local stable and unstable manifolds of $\mathcal{M}$;

- for suitably large values of κ we have the two periodic orbits of $\mathcal{M}_\kappa$ which are identified as halo orbits;

- for initial conditions close to the manifold tubes of the halo orbits we find orbits which approach the halo orbits from one side and then transit to the other side with a fly-by with the halo orbit (which we call the halo transit orbits), as well orbits which approach the halo orbits from one side and then bounce back.

Finally, the orbits found in the normal-form variables are mapped to the original Cartesian variables with the f-dependent canonical transformation

$$(\mathbf{q}, \mathbf{p}) = \mathcal{X}(\mathbf{Q}, \mathbf{P}; f)$$

conjugating the Hamiltonian (3) to the normal form (6). We remark that in the space of the Cartesian variables the halo orbits are transformed by $\mathcal{X}$ to quasi-periodic orbits; we call halo torus the set of all these periodic orbits.

3 Construction of the resonant Floquet-Birkhoff normal form

The resonant Floquet-Birkhoff normal form, as well as the canonical transformation from the Cartesian variables to the normal form variables, are represented as Taylor-Floquet expansions of terms proportional to

$$e^{i\nu f}\hat{q}_1^{m_1}\hat{q}_2^{m_2}\hat{q}_3^{m_3}\hat{p}_1^{l_1}\hat{p}_2^{l_2}\hat{p}_3^{l_3}$$

up to truncation orders $\mathcal{N}_1,\mathcal{N}_2$ for the polynomial variables and for the true anomaly:

$$m_1 + m_2 + m_3 + l_1 + l_2 + l_3 \leq \mathcal{N}_1 \quad , \quad |\nu| \leq \mathcal{N}_2 \ .$$

The coefficients of all these terms are represented in floating point numbers, obtained from an algebraic manipulator program performing the transformation to the normal form variables as the composition of:

(i) A canonical Floquet transformation:

$$(\mathbf{q}, \mathbf{p}) = \mathcal{C}(f; e)(\tilde{\mathbf{q}}, \tilde{\mathbf{p}})$$

conjugating the Hamiltonian (3) to an Hamiltonian:

$$\tilde{H}(\tilde{\mathbf{q}}, \tilde{\mathbf{p}}, f; e) = \tilde{H}_2(\tilde{\mathbf{q}}, \tilde{\mathbf{p}}; e) + \tilde{H}_3(\tilde{\mathbf{q}}, \tilde{\mathbf{p}}, f; e) + \dots \tag{10}$$

where each term $\tilde{H}_j(\tilde{\mathbf{q}}, \tilde{\mathbf{p}}, f; e)$ is polynomial of degree j in the variables $\tilde{\mathbf{q}}, \tilde{\mathbf{p}}$ and periodic in f with period 2π, while $\tilde{H}_2(\tilde{\mathbf{q}}, \tilde{\mathbf{p}}; e)$ is autonomous.

As it is well known, the Floquet transformation is not unique, since its definition depends on the arbitrary choice of a logarithm of the monodromy matrix associated to the equations of motion linearized at the Lagrange equilibrium. As pointed out in [28], the subsequent Birkhoff normalizations of Hamiltonian (10) perform much better if among all the possible Floquet transformations of (3) there is one which is close to the identity. Also in this paper we define the Floquet transformation for the ERTBP by selecting a close to the identity one, as shown in [28].

(ii) A linear canonical transformation:

$$(\tilde{\mathbf{q}}, \tilde{\mathbf{p}}) = \mathcal{D}(\hat{\mathbf{q}}, \hat{\mathbf{p}}) \tag{11}$$

giving $\tilde{H}_2(\tilde{\mathbf{q}}, \tilde{\mathbf{p}}; e)$ the normal form:

$$\hat{K}_2(\hat{\mathbf{q}}, \hat{\mathbf{p}}) = \sigma_1 \frac{\hat{q}_1^2 + \hat{p}_1^2}{2} + \sigma_2 \frac{\hat{q}_2^2 + \hat{p}_2^2}{2} + \lambda \hat{q}_3 \hat{p}_3. \tag{12}$$

We denote by $\hat{K}_j(\hat{\mathbf{q}}, \hat{\mathbf{p}}, f; e)$ the image of all the other polynomials $\hat{K}_j(\hat{\mathbf{q}}, \hat{\mathbf{p}}, f; e) = \tilde{H}_j(\mathcal{D}(\hat{\mathbf{q}}, \hat{\mathbf{p}}), f; e)$.

(iii) A sequence of $N - 2$ Birkhoff transformations giving the Hamiltonian the final resonant normal form (6).

The Floquet transformation (i) and the linear transformation $\mathcal{D}$ are discussed in [28], and require no modifications to adapt to the resonant case. Therefore we provide in this paper all the details of the resonant Birkhoff transformations (iii). The two linear transformations (i) and (ii) conjugate the Hamiltonian (3) to

$$\hat{H}(\hat{\mathbf{q}}, \hat{\mathbf{p}}, F, f) = F + \hat{H}_2(\hat{\mathbf{q}}, \hat{\mathbf{p}}) + \sum_{j \geq 3} \hat{H}_j(\hat{\mathbf{q}}, \hat{\mathbf{p}}, f; e) \ , \tag{13}$$

where the variable F, conjugated to f, has been introduced in order to conveniently deal with an autonomous Hamiltonian and the terms $\hat{H}_j$ for $j \geq 3$ are polynomials of degree j in the variables $\hat{\mathbf{q}}, \hat{\mathbf{p}}$ and periodic in f with period 2π. The terms $\hat{H}_j$ with $j \geq 3$ are represented as sum of monomials of the form

$$a_{\mathbf{m},\mathbf{l},\nu}^{(j)} e^{i\nu f} \hat{q}_1^{m_1} \hat{q}_2^{m_2} \hat{q}_3^{m_3} \hat{p}_1^{l_1} \hat{p}_2^{l_2} \hat{p}_3^{l_3} \ , \quad \sum_{i=1}^{3}(m_i + l_i) = j \ . \tag{14}$$

The objective of the resonant Birkhoff transformations is to tackle in a single algorithmic procedure two different effects: to remove the explicit dependence of $\hat{H}$ on f up to a large finite order N, and to define a normal form Hamiltonian which can be exploited to study the resonance generating the halo orbits. This is achieved with a close to the identity canonical transformation $\mathcal{C}_N$ conjugating the Hamiltonian (13), that now we denote as the initial Hamiltonian $\hat{H}^{(2)}$, to a normal form Hamiltonian

$$\hat{H}^{(N)} = F + \sum_{j=2}^{N} K_j^{(N)}(\hat{\mathbf{q}}, \hat{\mathbf{p}}) + \sum_{j \geq N+1} \hat{H}_j^{(N)}(\hat{\mathbf{q}}, \hat{\mathbf{p}}, f) \tag{15}$$

where the functions $K_j^{(N)}$ do not depend on F, f and are polynomials of degree j depending on $\hat{\mathbf{q}}, \hat{\mathbf{p}}$ only through monomials of the form:

$$a_{\mathbf{m}}^{(j,N)} \hat{q}_1^{m_1} \hat{q}_2^{m_2} \hat{q}_3^{m_3} \hat{p}_1^{l_1} \hat{p}_2^{l_2} \hat{p}_3^{l_3} \ , \tag{16}$$

with:

$$(l_1 - m_1) + (l_2 - m_2) = 0 \quad \text{and} \quad l_3 = m_3, \ \sum_{i=1}^{3} m_i + l_i = j \ . \tag{17}$$

The remainder terms $\hat{H}_j^{(N)}$ are polynomials of degree j with coefficients depending periodically on f with period 2π, represented as sum of monomials of the form

$$a_{\mathbf{m},\mathbf{l},\nu}^{(j,N)} e^{i\nu f} \hat{q}_1^{m_1} \hat{q}_2^{m_2} \hat{q}_3^{m_3} \hat{p}_1^{l_1} \hat{p}_2^{l_2} \hat{p}_3^{l_3} \ , \qquad \sum_{i=1}^{3}(m_i + l_i) = j \ . \tag{18}$$

The canonical transformation $\mathcal{C}_N$ is constructed from the composition of a sequence of $N - 2$ elementary canonical Birkhoff transformations. Precisely, we define the sequence of canonical transformations:

$$\mathcal{C}_J = \hat{\mathcal{C}}_{\chi_J} \circ \mathcal{C}_{J-1} \ , \quad J = 3, \ldots, N \tag{19}$$

conjugating $\hat{H} := \hat{H}^{(2)}$ to the intermediate Floquet-Birkhoff normal form Hamiltonians:

$$\hat{H}^{(J)} := \hat{H}^{(J-1)} \circ \mathcal{C}_J = F + \sum_{j=2}^{J} K_j^{(J)}(\hat{\mathbf{q}}, \hat{\mathbf{p}}) + \sum_{j \geq J+1} \hat{H}_j^{(J)}(\hat{\mathbf{q}}, \hat{\mathbf{p}}, f) \quad (20)$$

with the property that $K_j^{(J)}$ do not depend on F, f and are polynomials of degree j depending on $\hat{\mathbf{q}}, \hat{\mathbf{p}}$ only through monomials of the form (16) with powers satisfying (17), while $\hat{H}_j^{(J)}$ are polynomials of degree j with coefficients depending periodically on f with period 2π.

The transformations are defined as follows: $\mathcal{C}_2$ is the identity while $\hat{\mathcal{C}}_{\chi_J}$ is the Hamiltonian flow at time $f = 1$ of generating functions χ_J defined from the coefficients of $\hat{H}^{(J-1)}$. Below we describe the definition of the generating functions χ_J and the steps required for the algorithmic computation of each canonical transformation $\mathcal{C}_N$ and Hamiltonian $\hat{H}^{(N)}$ using the Lie series method (for an introduction to the method, see [6, 9]) and implemented with a computer algebra system in the examples presented in this paper. For each $J \geq 3$ we assume that the Hamiltonian $\hat{H}^{(J-1)}$ and the canonical transformation $\mathcal{C}_{N-1}$ are known, and we proceed as follows.

First, from $\hat{H}^{(J-1)}$ we compute the generating function χ_J:

$$\chi_J = \sum_{(\mathbf{m}, \mathbf{l}, \nu) \in \mathcal{L}_J} \frac{-a_{\nu, m_1, m_2, m_3, l_1, l_2, l_3}^{(J-1)}}{\mathrm{i}\,\sigma_1 (l_1 - m_1) + \mathrm{i}\,\sigma_2 (l_2 - m_2) + \lambda (l_3 - m_3) + \mathrm{i}\,\nu}\, \mathrm{e}^{\mathrm{i}\nu f}\, \hat{q}_1^{m_1} \hat{q}_2^{m_2} \hat{q}_3^{m_3} \hat{p}_1^{l_1} \hat{p}_2^{l_2} \hat{p}_3^{l_3} \quad (21)$$

where

$$\mathcal{L}_J = \left\{ (\mathbf{m}, \mathbf{l}, \nu) \in \mathbb{N}^3 \times \mathbb{N}^3 \times \mathbb{Z} : \sum_{j=1}^{3} (l_j + m_j) = J, \text{ and } |l_1 - m_1 + l_2 - m_2| + |l_3 - m_3| + |\nu| \geq 1 \right\}.$$

Next, we compute explicitly the canonical transformation

$$\hat{\mathcal{C}}_{\chi_J}(\hat{\mathbf{q}}^{(J)}, \hat{\mathbf{p}}^{(J)}, F^{(J)}, f^{(J)}) = (\hat{\mathbf{q}}^{(J-1)}, \hat{\mathbf{p}}^{(J-1)}, F^{(J-1)}, f^{(J-1)}) \,,$$

as the Lie series

$$\zeta = e^{L_{\chi_J}} \zeta' := \zeta' + \{\zeta', \chi_J\} + \frac{1}{2}\{\{\zeta', \chi_J\}, \chi_J\} + \dots \,, \quad (22)$$

where $L_{\chi_J} := \{\cdot, \chi_J\}$, and ζ, ζ' denote any couple of variables $\hat{\mathbf{q}}^{(J-1)}, \hat{\mathbf{q}}^{(J)}, \hat{\mathbf{p}}^{(J-1)}, \hat{\mathbf{p}}^{(J)}$ or $F^{(J-1)}, F^{(J)}$. The transformed Hamiltonian is computed as a Lie series as well:

$$\hat{H}^{(J)} = \hat{\mathcal{C}}_{\chi_J} \hat{H}^{(J-1)} = e^{L_{\chi_J}} \hat{H}^{(J-1)}. \quad (23)$$

The iteration ends for $J = N$, and finally, by reintroducing real canonical variables,

$$\begin{aligned}
\hat{q}_1^{(N)} &= \frac{Q_1 - \mathrm{i}\, P_1}{\sqrt{2}} \,, & \hat{p}_1^{(N)} &= \frac{P_1 - \mathrm{i}\, Q_1}{\sqrt{2}} \,, \\
\hat{q}_2^{(N)} &= \frac{Q_2 - \mathrm{i}\, P_2}{\sqrt{2}} \,, & \hat{p}_2^{(N)} &= \frac{P_2 - \mathrm{i}\, Q_2}{\sqrt{2}} \,, \\
\hat{q}_3^{(N)} &= Q_3 \,, & \hat{p}_3^{(N)} &= P_3 \,,
\end{aligned} \quad (24)$$

and by suitably identifying the terms $\hat{K}_j$ with K_j, and disregarding the dummy action $F^{(N)}$, we recover the final Floquet-Birkhoff normal form as in Eq. (6).

4 Resonant dynamics in the center manifold of the elliptic Earth-Moon system

In this Section we illustrate the use of the resonant Floquet-Birkhoff normal forms to represent the dynamics related to the halo orbits in a model problem, which we identify as the Earth-Moon ERTBP. The relevance of the Earth-Moon halo orbits for the space-flight dynamics has been considered in several papers [10, 25, 19, 35]. The basic model to study the dynamics of a spacecraft in the Earth-Moon system is the Circular Restricted Three-Body Problem (CRTBP) with the Earth and the Moon as primaries. This model, although simplistic compared to the model of the Solar System which is considered to compute modern ephemerides, had nevertheless provided deep insights regarding the dynamics of small bodies in the Solar System.

For the value of $\mu = 0.0123$ and $e = 0.0549006$ considered in the present paper (representing the Earth-Moon ERTBP), after 4 normalization steps ($N = 6$), the normal form $K(\mathbf{Q}, \mathbf{P}; e)$ introduced in (6) takes the form:

$$K(\mathbf{Q}, \mathbf{P}; e) = K_2(\mathbf{Q}, \mathbf{P}; e) + K_4(\mathbf{Q}, \mathbf{P}; e) + K_6(\mathbf{Q}, \mathbf{P}; e) + R_7(\mathbf{Q}, \mathbf{P}, f; e)$$

where

$$
\begin{aligned}
K_2(\mathbf{Q}, \mathbf{P}; e) =\ & 2.33662\,\frac{Q_1^2 + P_1^2}{2} + 2.27111\,\frac{Q_2^2 + P_2^2}{2} + 2.93590\,Q_3\,P_3\ , \\
K_4(\mathbf{Q}, \mathbf{P}; e) =\ & -1.76908\,P_1^4 + 1.74292\,P_1^2\,P_2^2 - 1.58163\,P_2^4 - 3.53816\,P_1^2\,Q_1^2 \\
& -3.33654\,P_2^2\,Q_1^2 - 1.76908\,Q_1^4 + 10.15894\,P_1\,P_2\,Q_1\,Q_2 - 3.33654\,P_1^2\,Q_2^2 \\
& -3.16326\,P_2^2\,Q_2^2 + 1.74292\,Q_1^2\,Q_2^2 - 1.58163\,Q_2^4 - 16.44122\,P_1^2\,P_3\,Q_3 \\
& -15.03657\,P_2^2\,P_3\,Q_3 - 16.44122\,Q_1^2\,P_3\,Q_3 - 15.03657\,Q_2^2\,P_3\,Q_3 - 9.57863\,P_3^2\,Q_3^2 \\
K_6(\mathbf{Q}, \mathbf{P}; e) =\ & -3.13968\,P_1^6 + 6.82217\,P_1^4\,P_2^2 + 5.97758\,P_1^2\,P_2^4 - 1.99158\,P_2^6 \\
& -9.41904\,P_1^4\,Q_1^2 - 1.38474\,P_1^2\,P_2^2\,Q_1^2 - 7.06430\,P_2^4\,Q_1^2 - 9.41905\,P_1^2\,Q_1^4 \\
& -8.20691\,P_2^2\,Q_1^4 - 3.13968\,Q_1^6 + 30.05816\,P_1^3\,P_2\,Q_1\,Q_2 + 26.08374\,P_1\,P_2^3\,Q_1\,Q_2 \\
& +30.05816\,P_1\,P_2\,Q_1^3\,Q_2 - 8.20690\,P_1^4\,Q_2^2 - 1.08671\,P_1^2\,P_2^2\,Q_2^2 - 5.97474\,P_2^4\,Q_2^2 \\
& -1.38473\,P_1^2\,Q_1^2\,Q_2^2 - 1.08671\,P_2^2\,Q_1^2\,Q_2^2 + 6.82217\,Q_1^4\,Q_2^2 + 26.08374\,P_1\,P_2\,Q_1\,Q_2^3 \\
& -7.06430\,P_1^2\,Q_2^4 - 5.97474\,P_2^2\,Q_2^4 + 5.97758\,Q_1^2\,Q_2^4 - 1.99158\,Q_2^6 \\
& -11.98956\,P_1^4\,P_3\,Q_3 - 96.12101\,P_1^2\,P_2^2\,P_3\,Q_3 - 3.55055\,P_2^4\,P_3\,Q_3 \\
& -23.97913\,P_1^2\,P_3\,Q_1^2\,Q_3 - 15.47041\,P_2^2\,P_3\,Q_1^2\,Q_3 - 11.98956\,P_3\,Q_1^4\,Q_3 \\
& -161.30118\,P_1\,P_2\,P_3\,Q_1\,Q_2\,Q_3 - 15.47041\,P_1^2\,P_3\,Q_2^2\,Q_3 - 7.10110\,P_2^2\,P_3\,Q_2^2\,Q_3 \\
& -96.12101\,P_3\,Q_1^2\,Q_2^2\,Q_3 - 3.55055\,P_3\,Q_2^4\,Q_3 - 105.42195\,P_1^2\,P_3^2\,Q_3^2 \\
& -70.52337\,P_2^2\,P_3^2\,Q_3^2 - 105.42195\,P_3^3\,Q_1^2\,Q_3^2 - 70.52337\,P_3^2\,Q_2^2\,Q_3^2 \\
& -54.46117\,P_3^3\,Q_3^3
\end{aligned}
$$

We exploit the tailored constructed resonant normal form in order to compute the halo orbits, for a certain value of the local energy. First, we analyze the dynamics on the center manifold by computing its Poincaré surfaces of section. We denote by $\hat{K}_{CM}(Q_1, Q_2, P_1, P_2; e)$

the 2-degrees of freedom Hamiltonian of the system restricted to the center manifold, expressed with the real canonical variables $\mathbf{Q}, \mathbf{P}$ (as a matter of fact, only Q_1, Q_2, P_1, P_2 are needed):

$$
\begin{aligned}
K_{CM}(Q_1, Q_2, P_1, P_2; e) &:= K(Q_1, Q_2, 0, P_1, P_2, 0; e) \\
&:= K_{CM,2}(Q_1, Q_2, P_1, P_2; e) + K_{CM,4}(Q_1, Q_2, P_1, P_2; e) + .
\end{aligned} \tag{25}
$$

For fixed values κ of the local energy, we consider the Poincaré section defined by the flow of K_{CM} and the surface:

$$
\Sigma_\kappa = \{(Q_1, Q_2, P_1, P_2): \quad K_{CM}(Q_1, Q_2, P_1, P_2; e) = \kappa \quad , \quad Q_2 = 0, \quad P_2 > 0\}, \tag{26}
$$

which is parameterized by the variables Q_1, P_1. In figure 2 we represent a sample of these Poincaré sections numerically computed for increasing values of the local energy $\kappa = 0.005, 0.025, 0.050, 0.077$; in figure 3 we represent these Poincaré sections in the space of the Cartesian variables, via the transformation (2) computed for $Q_2, Q_3, P_3, f = 0$. In the phase-portraits of the Poincaré sections we identify the following families of peculiar motions[1]

- **Vertical Lyapunov tori:** Since $\hat{K}_2, \hat{K}_4, \hat{K}_6$ do not contain monomials with $l_1 = 1, m_1 = 0$ or $l_1 = 0, m_1 = 1$, the origin $(Q_1, P_1) = (0, 0)$ is a fixed point of all the Poincaré sections, corresponding to a periodic orbit in the family of the vertical Lyapunov orbits. Since the canonical transformation $\mathcal{X}(\mathbf{Q}, \mathbf{P}, f; e)$ maps these periodic orbits to tori of the Cartesian space, the origin of the Poincaré sections provides the family of vertical Lyapunov tori.

- **Planar Lyapunov tori:** The borders of the Poincaré sections (which, strictly speaking, do not belong to the section Σ_κ), which are obtained for the limit initial conditions $(Q_2, P_2) = 0$ and Q_1, P_1 satisfying:

$$
K_{CM}(Q_1, 0, P_1, 0; e) = \kappa,
$$

correspond to the family of the planar Lyapunov orbits, which are mapped to the planar Lyapunov tori of the Cartesian space. In fact, since $\hat{K}_2, \hat{K}_4, \hat{K}_6$ do not contains monomials with $l_2 = 1, m_2 = 0, l_3, m_3 = 0$ or $l_2 = 0, m_2 = 1, l_3, m_3 = 0$, each solution of the Hamilton equations of K_{CM} with $(Q_2(0), P_2(0)) = (0, 0)$, satisfies $(Q_2(t), P_2(t)) = (0, 0)$ for all t, thus providing a planar periodic orbit. Since the canonical transformation $\mathcal{X}(\mathbf{Q}, \mathbf{P}, f; e)$ maps these orbits to tori of the Cartesian space, the limit border of the Poincaré section provides the family of planar Lyapunov tori. We remark that both the planar and vertical Lyapunov tori are more efficiently computed with the non-resonant normal forms defined in the paper [28].

---

[1]The following description refers to the flow which is obtained from the Hamiltonian of the ERTBP by neglecting the remainder R_7 in the Floquet-Birkhoff normal form. When considering the non approximated flow of the elliptic restricted three-body problem, the description is affected by an error which is discussed in Sections 4.1 and 4.2.
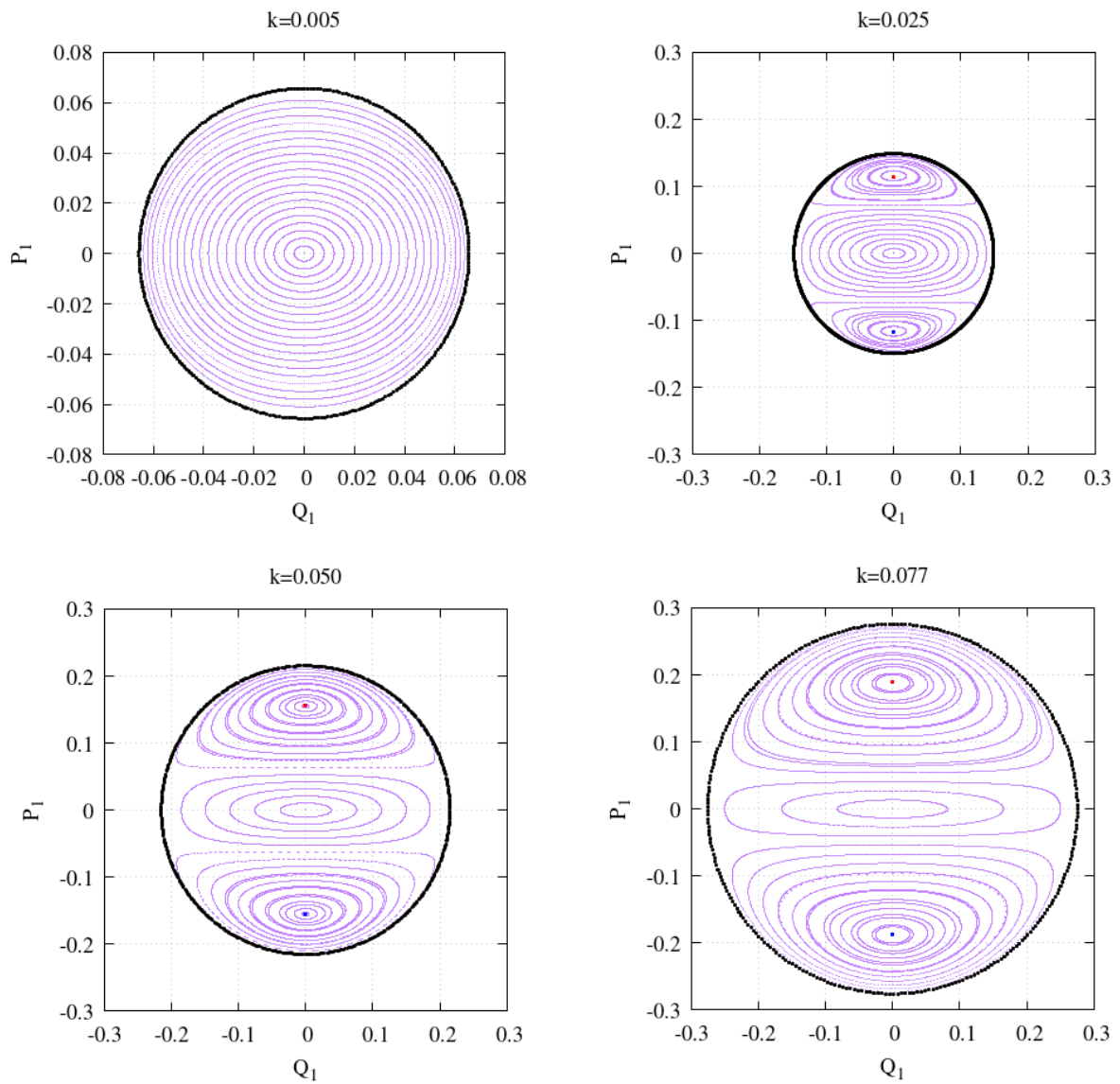
Figure 2: Representation of the Poincaré sections of the flow on the center manifold originating at the Lagrangian solution L_1 of the Earth-Moon system, for a sample of values of the local energy κ, in the plane of the normal form variables Q_1, P_1.

- **Halo tori.** We identify the halo orbits of the ERTBP as the fixed points of the Poincaré section of the Hamiltonian system defined by K_{CM} (which appear in addition to the central one identified by $(Q_1, P_1) = (0, 0)$) for all the larger values of the local energy $\kappa = 0.025, 0.050, 0.077$. As for the CRTBP (see [24, 2, 29]), the halo orbits are better described by introducing normal form variables which are adapted to the 1-1 resonance. First, we introduce on the center manifold the action-angle variables $\theta_1, \theta_2, I_1, I_2$ defined in (8), and then the action-angle variables $\phi, \chi, J_\phi, J_\chi$ adapted to the 1-1 resonance defined by:

$$
\begin{aligned}
\theta_1 &= \phi + \chi , & \theta_2 &= \chi \\
I_1 &= J_\phi , & I_2 &= J_\chi - J_\phi .
\end{aligned}
\tag{27}
$$

Since the representation of the Hamilton function K_{CM} in the action-angle variables does not depend on the angle χ, the conjugate action J_χ is a first integral and the motion of the couple ϕ, J_ϕ is computed from the 1-degree of freedom reduced Hamiltonian system obtained for fixed values of J_χ. The halo orbits are computed as the equilibrium points of the reduced system, and correspond to fixed points of the Poincaré section with $Q_1 = 0, P_1 \neq 0$. Because the action-angle variables ϕ, J_ϕ are singular for $J_\phi = 0$, the computation of the equilibrium points of the reduced system is better performed using the non-singular canonical variables:

$$
\tilde{x} = \sqrt{2 J_\phi} \sin \phi , \qquad \tilde{y} = \sqrt{2 J_\phi} \cos \phi .
\tag{28}
$$

Therefore, by computing K_{CM} in the variables $\chi, J_\chi, \tilde{x}, \tilde{y}$ we obtain a function:

$$
\tilde{K}_{CM} := \tilde{K}_{CM}(J_\chi, \tilde{x}, \tilde{y})
$$

which is a polynomial of order 6 in the variables $\tilde{x}, \tilde{y}$, with coefficients depending polynomially on J_χ (up to order 3). We therefore proceed by computing the equilibrium points of the reduced Hamiltonian $\tilde{K}_{CM}$ with $\tilde{x} = 0, \tilde{y} \neq 0$, and the corresponding initial conditions on the Poincaré section obtained for $\chi = 0$. Finally, we remark that the equilibrium points of the reduced system provide periodic orbits in the center manifold, which are projected to families of quasi-periodic orbits of the Cartesian space, which we call the family of halo tori of the ERTBP.

Therefore the halo orbits obtained for large order approximations of the ERTBP, as it happens with the Lyapunov orbits, are quasi-periodic orbits belonging to 2-dimensional tori. In figure 4 we represent in the space of the Cartesian variables x, y, z the projections of both the Poincaré section and the (southern and northern) families of the corresponding halo tori computed for $f = 0$ and for $\kappa = 0.025, 0.05$ (left and right panels respectively). As expected, the halo section of the halo tori for $f = 0$ cross the Poincaré section in the corresponding fixed point.

4.1 Validation of the halo orbits and the halo manifold tubes

In order to test that the orbits generated from the normal form computations are a good representation of the dynamics of the full ERTBP, and to determine the effects of
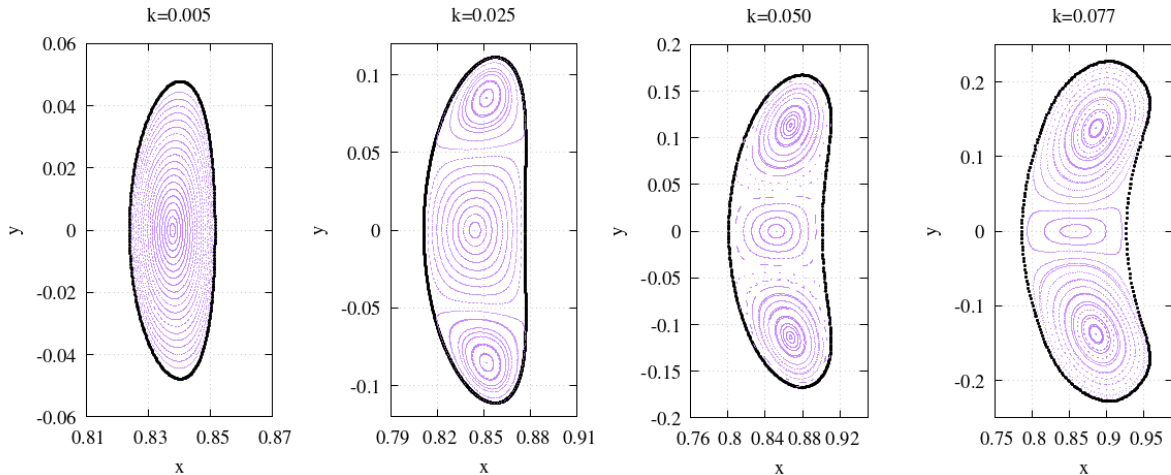
Figure 3: Representation of the same Poincaré sections of fig. 2 in the plane of the Cartesian coordinates x, y, computed by transforming the values of the normal form variables for $f = 0$. The thick black curve corresponds to the section $f = 0$ of the planar Lyapunov torus.

eventual small errors, we perform the following validation test. Along with the section of the halo tori for $f = 0$, we first compute the sections of the torus for other values of f, namely $f = \pi$, $f = \pi/2$, using the Hamiltonian flow of K_{CM}. When transformed to Cartesian variables x, y, z, these sections provide a segmented depiction of the halo torus in the 3 dimensional space. Then, we numerically integrate the initial conditions of the halo orbits (transformed to Cartesian variables) using a numerical integrator of the full ERTBP represented by Hamiltonian (1). Since the halo torus is hyperbolic in the normal form dynamics, we expect that the small errors introduced by neglecting the remainder R_{N+1} are responsible of an hyperbolic drift of the numerically computed orbit from the analytically computed halo torus. As usual with hyperbolic dynamics, even if for small values of the norm of R_{N+1} the errors on the initial conditions are small, this small error grows exponentially in time. As it happens for the computation of the Lyapunov orbits of the CRTBP, the hyperbolic components is so strong that typically the numerically integrated orbits depart from the analytically computed ones within few periods. We check for how long the evolution of the numerically computed halo orbits remains close to the corresponding analytically computed halo torus for a value of the local energy $\kappa = 0.025$. In Figure 5 we represent a numerically integrated orbit which remains close to the torus for a full circulation before departing exponentially from it. As expected, the larger is the local energy energy, the larger is the amplitude of the corresponding halo torus and the shorter is the time required for the orbit to depart from it. We also represent with a color scale the variation of the value of the local energy κ during the numerical integration, which represents the best estimator of the error. In fact, the variation of the local energy remains small also when the orbit departs form the torus. The exponential instability of individual orbits provides an opportunity to construct orbits of the full ERTBP which arrive close to (or depart from) the halo torus or that transit close to it, as it has been done in correlation with the Lyapunov tori of the ERTBP previously studied

15
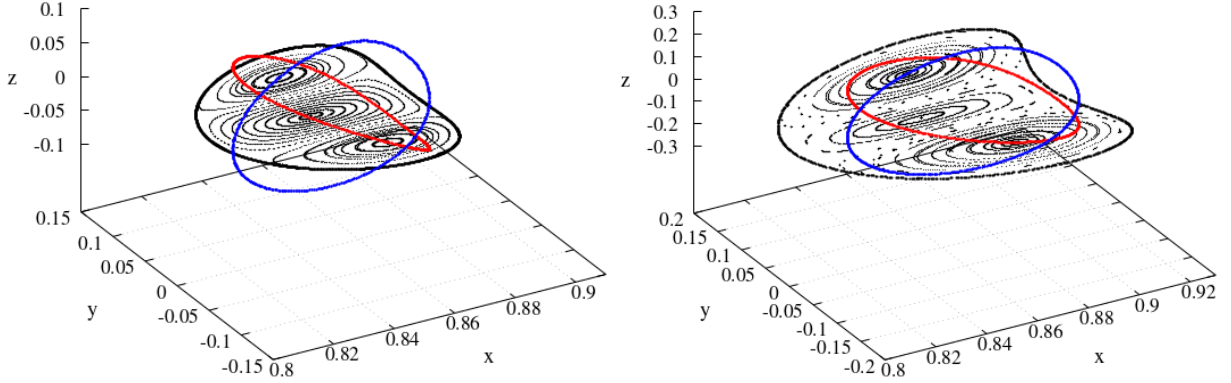
Figure 4: Representation in the space of the Cartesian variables x, y, z of the Poincaré sections and the projection of the (southern and northern) families of the corresponding halo tori computed for $f = 0$ and for $\kappa = 0.025, 0.05$ (left and right panels respectively).

in [28]. A sample of numerically computed orbits in the stable and unstable halo tubes, whose initial conditions have been obtained using the Floquet-Birkhoff normal form, is represented in Figure 6.

4.2 The remainder R_{N+1}

Another validation test is performed with a direct computation of the norm of the remainder R_{N+1} of the Floquet-Birkhoff normal form (6) along the halo orbit, as well as in a neighbourhood. In fact, since the halo tori are characterized by large librations from the corresponding Lagrangian solution, it is important to check that the remainder R_{N+1} (which is neglected in the definition of the torus) is indeed small in a neighbourhood of the torus. Previously we have checked with an indirect method the norm of the remainder by computing the variation of the local energy along a numerically integrated solution of the ER3BP. Now we represent a direct computation of the norm of the remainder computed along different halo tori and different normalizations orders.

We first define the maximum of the norm of the remainder on a set of points $\mathcal{S}$ as

$$|R^{(J)}| := \text{Max}_{(\hat{\mathbf{q}}, \hat{\mathbf{p}}, f) \in \mathcal{S}} \sum_{j=J+1}^{10} |\hat{H}_j^{(J)}(\hat{\mathbf{q}}, \hat{\mathbf{p}}, f)| , \qquad (29)$$

for all the normalization orders $J = 2, \ldots, N$, and then we compute it on a set $\mathcal{S}$ of points sampling the Halo orbits. The results are summarized in Table 1, and show the orders of magnitude of improvement in the error of our best Floquet-Birkhoff normal form (of order $J = 8$) with respect to the classical Floquet approximation where no Birkhoff transformations are implemented (corresponding to order $J = 2$).

Let us remark that the an effect of the error introduced by truncating the remainder is that for the orbits with initial conditions which are on the halo orbits evolve as the orbits which are in a small neighbourhood of the stable and unstable manifold tubes. According the the position of the initial values of the hyperbolic variables with respect

16
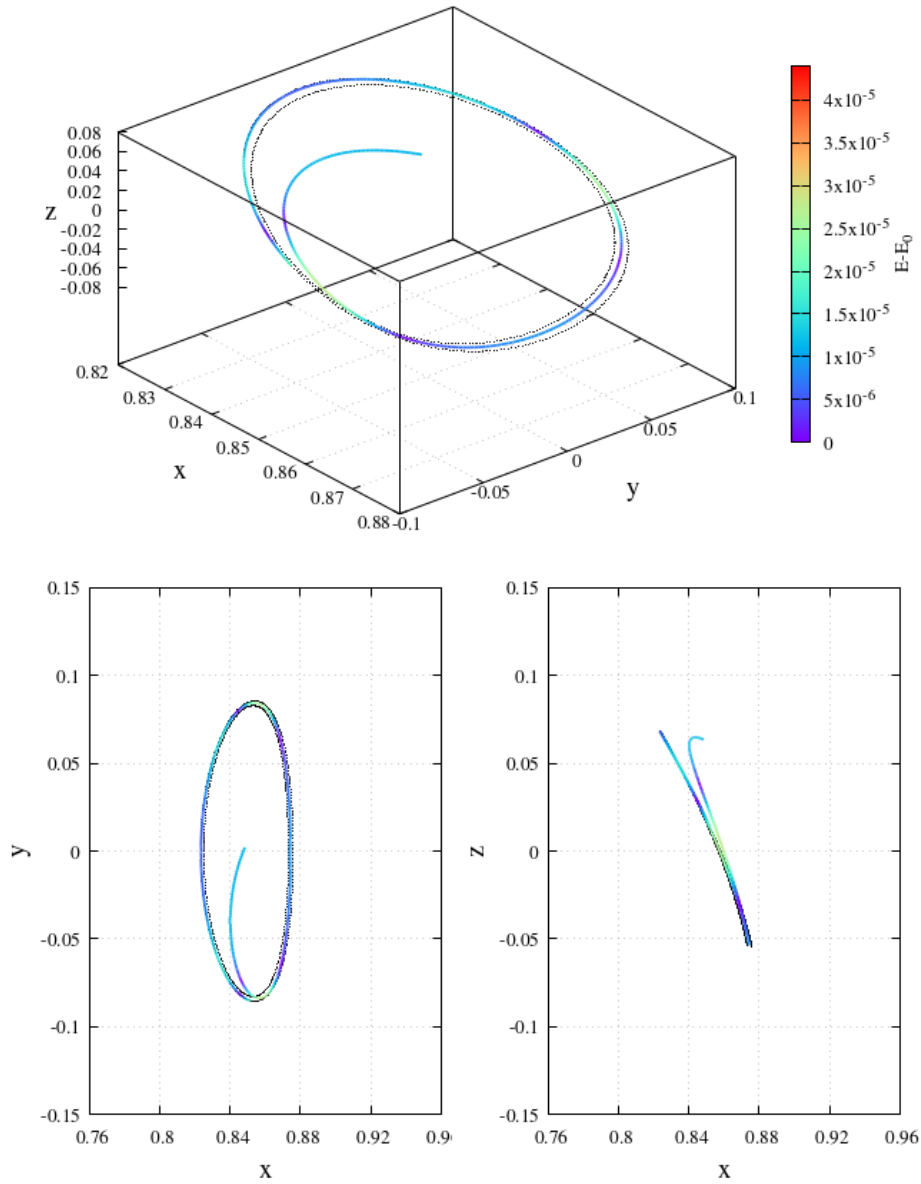
Figure 5: A solution of the ERTBP computed by numerically integrating the Hamilton equations of (1) with an initial condition on the northern halo torus, for $\kappa = 0.0025$. The black points belong to sections of the torus computed for $f = 0$ (the external one) and $f = \pi$ (the internal one). The numerically computed orbit (colored curve) moves close the f-section of the Halo torus before departing exponentially from it. The upper panel represents the orbit in the xyz space, the lower panels the projections on the xy (left) and xz (right) planes. The color on the orbits represent the variation of the local energy, providing an estimate of the neglected remainder of the Floquet-Birkhoff normal form along the solution.

17
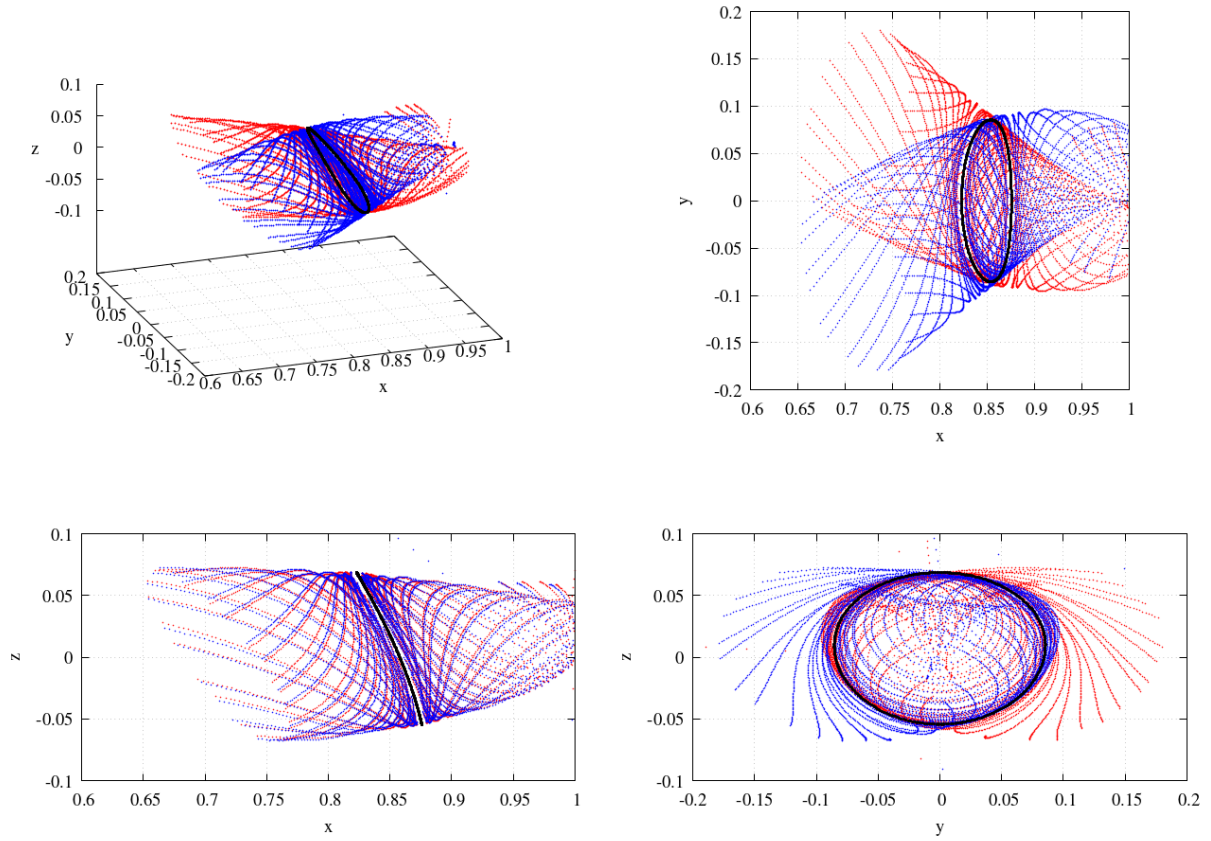
Figure 6: A sample of numerically computed orbits in the stable (blue) and unstable (red) halo tubes, whose initial conditions have been obtained using the Floquet-Birkhoff normal form, for $\kappa = 0.025$. The black dots are in the halo torus.

$\mu = 0.012300$ $e = 0.0549006$ (Earth-Moon system)					
Center manifold Halos					
Halo for $\kappa = 0.025$		Halo for $\kappa = 0.030$		Halo for $\kappa = 0.050$	
J	$|R^{(J)}|$	J	$|R^{(j)}|$	J	$|R^{(j)}|$
2	1.45043×10^{-2}	2	2.39118×10^{-2}	2	1.12098×10^{-1}
3	1.42105×10^{-3}	3	2.39449×10^{-3}	3	1.08179×10^{-2}
4	5.40381×10^{-4}	4	9.88391×10^{-4}	4	5.55895×10^{-3}
5	2.58946×10^{-4}	5	5.10725×10^{-4}	5	3.48433×10^{-3}
6	1.09358×10^{-4}	6	2.33717×10^{-4}	6	1.96300×10^{-3}
7	4.41467×10^{-5}	7	1.01352×10^{-4}	7	1.02467×10^{-3}
8	1.47660×10^{-5}	8	3.60189×10^{-5}	8	4.25978×10^{-4}

Table 1: Estimation of the norm of the remainder (29) for the three halo orbits of previous section, for energies $\kappa = 0.025$, $\kappa = 0.030$, $\kappa = 0.050$.

to the values of the stable and unstable tubes provides orbits which have different transit properties at the halo orbits. In figure 7 we represent orbits which are very close to the stable and unstable tubes, but after they approach the halo torus, depending on their position relative to the tubes they transit from one side to the other of the halo torus, or instead they bounce back. We therefore find the same kind of transits behaviour that has been previously found for the planar Lyapunov orbits.

Acknowledgments
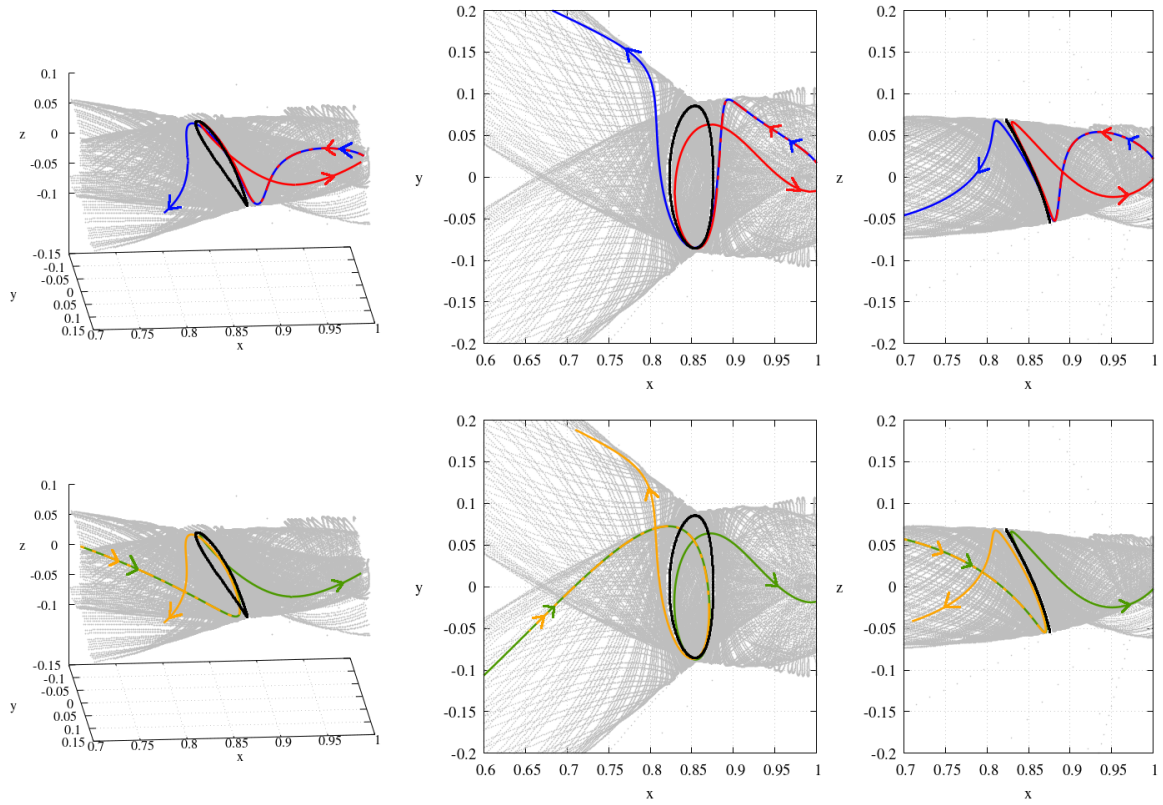
Figure 7: Numerically computed orbits in the stable and unstable halo tubes (in gray), together with orbits which transit from one side of the halo torus to the other, or bounce back. The initial conditions of all these orbits have been obtained using the Floquet-Birkhoff normal form, for $\kappa = 0.025$, the black dots are in the halo torus.

References

[1] Arnold, V.I., (1963) Proof of a theorem of A.N. Kolmogorov on the invariance of quasi-periodic motions under small perturbations of the Hamiltonian, *Usp. Mat. Nauk.* **18** p 13, *Russ. Math. Surv.* **18**, p 9.

[2] Ceccaroni M., Celletti A., Pucacco G., Halo orbits around the collinear points of the restricted three-body problem. *Physica D* **317**, p 28 (2016).

[3] Dei Tos, D.A., Topputo, F., Trajectory refinement fo the three-body orbits in the Real Solar System Model, *Adv. Space Research* **59**, p 2117 (2017)

[4] Celletti, A., Pucacco, G., Stella, D., Lissajous and Halo orbits in the Restricted Three-Body Problem, *J. Nonlinear Sci* **25**, p 343 (2015)

[5] Efthymiopoulos C., Giorgilli A., Contopoulos G., Nonconvergence of formal integrals II: Improved estimates for the optimal order of truncation, *J. Phys. A* **37**, p 10831 (2004).

[6] Efthymiopoulos C., Canonical perturbation theory, stability and diffusion in Hamiltonian systems: applications in dynamical astronomy, in *3rd La Plata International School on Astronomy and Geophysics "Chaos, Diffusion and Non-integrability in Hamiltonian Systems - Aplications to Astronomy"* (1st edition), Cincotta, P., Giordano, C., Efthymiopoulos, C., *eds.*, Uni. Nac. de la Plata, La Plata (2011).

[7] Farquhar R.W., The utilization of Halo orbits in advanced lunar operations, *NASA Tech. Notes* **D-6365** (1971).

[8] Farquhar R.W., A Halo-orbit lunar station, *Astronaut. Aeronaut.* p 59 (1972).

[9] Giorgilli A., Notes on exponential stability of Hamiltonian systems, in Dynamical Systems. Part I: Hamiltonian Systems and Celestial Mechanics (1st edition), *Pubblicazioni della Classe di Scienze, Scuola Normale Superiore, Centro di Ricerca Matematica "Ennio De Giorgi"*, Pisa (2003).

[10] Gómez G., Jorba À., Masdemont J., Simó C., Study of the transfer from the Earth to a Halo orbit around the equilibrium point L_1, *Celest. Mech. Dyn. Astron* **56**, p 541 (1993).

[11] Gómez G., Masdemont J.J., Mondelo J.M., Dynamical substitutes of the libration points for simplified solar system models, *Libration Point Orbits and Appl.* p 373 (2003).

[12] Gómez G., Mondelo J.M., The dynamics around the collinear equilibrium points of the RTBP, *Physica D*, **157** p 283 (2001).

[13] Hou X.Y., Liu L., On quasi-periodic motions around the collinear libration points in the real Earth-Moon system, *CMDA* **110**, p 71 (2011).

[14] Howell K.C., Three-dimensional, periodic, 'Halo' orbits, *Celest. Mech. Dyn. Astron.* **32**, p 53 (1984).

[15] Howell K.C., Families of Orbits in the Vicinity of the Collinear Libration Points, *J. Astronaut. Sci.* **49**, p 107 (2001).

[16] Jorba A., Masdemont J., Dynamics in the center manifold of the restricted three-body problem, *Physica D* **132**, p 189 (1999).

[17] Jorba A., Jorba-Cuscó M., Rosales J.J., The vicinity of the Earth-Moon L_1 point in the bicircular problem, *Celest. Mech. Dyn. Astron.* **32**, p 11 (2020).

[18] Kolmogorov, A.N., (1954) Preservation of conditionally periodic movements with small change in the Hamiltonian function, *Dokl. Akad. Nauk. SSSR* **98**, p 527.

[19] Koon W.S., Lo M.W., Marsden J.E., Ross S.D., Dynamical Systems, the three body problem and space mission design. *Marsden Books*. ISBN 978-0-615-24095-4 (2008).

[20] Lei H., Xu B., Hou X., Sun Y., High-order solutions of invariant manifolds associated with libration point orbits in the elliptic restricted three-body problem, *CMDA* **117**, p 349 (2013).

[21] Lian Y., Gómez G., Masdemont J.J., Tang G., A note on the dynamics around the Lagrange collinear points of the Earth-Moon system in a complete Solar System model, *CMDA* **115**, p 185 (2013).

[22] Luo Z-F., Topputo F., Bernelli-Zazzera F., Tang G-J., Constructing ballistic capture orbits in the real Solar System model, *CMDA* **120**, p 433 (2014).

[23] MacCarthy B.P., Howell C., Quasi-Periodic orbits in the Sun-Earth-Moon Bicircular Restricted Four-Body Problem, *AAS* **21**, p 270 (2021).

[24] Marchesiello A., Pucacco G., Resonances and bifurcations in systems with elliptical equipotentials, *MNRAS* **428**, p 2029 (2012).

[25] Masdemont J.J., High Order Expansions of Invariant Manifolds of Libration Point Orbits with Applications to Mission Design, *Dyn. Syst.*, **20**(1), p 59 (2005).

[26] Moser, J., (1962) On invariant curves of area-preserving mappings of an annulus, *Nachr. Akad. Wiss. Gött. II Math. Phys.* **KI**, p 1.

[27] Páez R.I., Guzzo M., A study of temporary captures and collisions in the Circular Restricted Three-Body Problem with normalizations of the Levi-Civita Hamiltonian, *I. J. Nonl. Mech.* **120**, p 103417 (2020).

[28] Páez R.I., Guzzo M., Transits close to the Lagrangian solutions L_1, L_2 in the elliptic restricted three-body problem, *Nonlinearity* **34**(9), p 6417 (2021).

[29] Pucacco G., Structure of the centre manifold of the L_1, L_2 collinear libration points in the restricted three-body problem, *Cel. Mech. and Dyn. Astr.* **131**, art. 44 (2019).

[30] Qian Y-J., Guo J-Y., Yu T-J., Yang X-D., Wang D-M., Halo orbits construction based on invariant manifolds technique, *Acta Astronautica* **163**, p 24 (2019).

[31] Qian Y., Yan X., Jing W., Zhang W., An improved numerical method for constructing Halo/Lissajous orbits in a full solar system model, *Chin. J. Aeronaut.* **31**, p 1362 (2018).

[32] Rosales, J.J., Jorba, A., Jorba-Cuscó, M., Families of Halo-like invariant tori around L_2 in the Earth-Moon Bicircular Problem, *CMDA* **133**, p 1 (2021)

[33] Scantamburlo E., Guzzo M., Short-period effects of the planetary perturbations on the Sun-Earth Lagrangian point L_3, *Astron. Astrophys.* **638**, A137 (2020).

[34] Scantamburlo, E., Guzzo, M., Paez, R.I., Interplanetary transfers using stable and unstable manifold tubes originating at L1 and L2 in the elliptic restricted three body problems, *preprint* https://hal.archives-ouvertes.fr/hal-03436121/ (2021).

[35] Zanzottera A., Castelli R., Mingotti G., Dellnitz M., Intersecting invariant manifolds in spatial restricted three-body problems: Design and optimization of Earth-to-halo transfers in the Sun-Earth-Moon scenario, *Commun. Nonlin. Science Num. Sim.* **17**(2), p 832 (2012).